Pergamon

Bioorganic & Medicinal Chemistry 9 (2001) 1293–1305

BIOORGANIC & MEDICINAL CHEMISTRY

Theoretical Investigation of (−)1-(Benzofuran-2-yl)-2-propylaminopentane [(−)-BPAP] as a Hydroxyl Radical Scavenger

Sachiko Nakai and Fumio Yoneda*

Fujimoto Pharmaceutical Corporation, 1-3-40 Nishi-Otsuka, Matsubara-shi, Osaka 580-8503, Japan

Received 12 October 2000; accepted 28 December 2000

Abstract—The chemical reactions between (−)-BPAP and •OH were studied using molecular orbital theory, with several simplified models. (−)-BPAP was proved to be a good radical scavenger. It was found that every atom of the benzofuran ring, except carbon 3, was capable of easily trapping the radical, where the most active site was carbon 1 on the furan part. The activation energies for the trappings were ca. 10 kcal/mol by the calculations at UHF/6-31G(d)//UHF/3-21G level. Since the single radical trapping products were still radicals, these could trap further radicals by way of cascade without any activation energy. Thus, the double radical trapping products were very stable, of which the lowest energy level was about 80 kcal/mol lower than the starting reactants.

Introduction

Recent theoretical study[1] of (−)-deprenyl (selegiline) suggested that this drug might be useful as a neuroprotective agent for neurodegenerative diseases concerned with possible oxidative damages in the central nervous system (CNS). (−)-Deprenyl has, theoretically, turned out to be a good and effective scavenger for the neurotoxic radical such as hydroxyl radical (•OH), for which the active site was its acetylenic part. (−)-Deprenyl has originally been known as a potent selective inhibitor of B-type monoamine oxidase (MAO-B) and later as a catecholaminergic/seretoninergic activity enhancer (CAE/SAE) substance.[2] The CAE/SAE effect is considered to be involved in the beneficial pharmacological effect of (−)-deprenyl in the treatment of Parkinson's disease,[3] in addition to the effect of MAO-B inhibition.

We have recently developed (−)1-(benzofuran-2-yl)-2-propylaminopentane, (−)-BPAP, a highly potent and selective CAE/SAE substance, as a potential follower of (−)-deprenyl in clinic, and it is a promising experimental tool for the analysis of the CAE/SAE mechanism.[4] It is interesting to note that (−)-BPAP has no acetylenic part and no MAO-B inhibitory activity in contrast to (−)-deprenyl. Incidentally, naturally occurring furan fatty acids have been shown to have the •OH scavenging activity.[5] The above information led us to theoretically examine whether (−)-BPAP could serve as a scavenger for •OH, like (−)-deprenyl. This article describes a quantum chemical investigation of the reactions between (−)-BPAP and •OH using several simplified models.

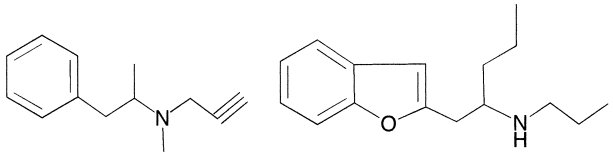

(-)-Deprenyl (-)-BPAP

Chart 1.

Computational Method

The geometry optimizations were calculated by ab initio molecular orbital theory using the GAUSSIAN94 program.[6] The results presented here are mainly based on method A by Hartree-Fock self-consistent field theory (HF), HF/6-31G(d)//HF/3-21G. Some calculations were done by method B, which is designated for the second

*Corresponding author. Tel.: +81-723-32-5151; fax: +81-723-8482; e-mail: soyaku@fujimoto-pharm.co.jp

0968-0896/01/$ - see front matter
PII: S0968-0896(01)00008-6

order Møller–Plesset perturbation theory[7] (MP2), MP2/6-31G(d)//MP2/3-21G, or by method C which is designated for the density functional theory[8] (DFT)-B3LYP method, B3LYP/6-31G(d)//B3LYP/3-21G, in order to confirm the results by method A, because in the calculations by method A for the radical systems, the spin contaminations were large. In methods A, B, and C, the optimizations were done at 3-21G level and then the single point calculations for the energy and the densities were done at 6-31G(d) level. Some optimizations were carried out at the 6-31G(d) level. The restricted method (RHF, MP2 or B3LYP) was used for closed-shell systems and the unrestricted method (UHF, UMP2 or UB3LYP) was for radical open-shell systems. The atomic charge densities were calculated by Mulliken population analysis. The frequency analysis in the Gaussian program was employed for the verifications of the transition states.

Configurations and frontier molecular orbitals of (−)-BPAP and models

The configurations optimized for the systems (−)-BPAP, BF1, BF2 and BF3 and their frontier molecular orbitals are represented in Figure 1. BF1, BF2 and BF3 were taken as the simplified models of (−)-BPAP. The numbers in Figure 1 are the energy levels of the orbitals in atomic unit. The frontier orbitals of these systems were very similar to each other and it is observed that both the highest occupied molecular orbitals (HOMOs) and the lowest unoccupied molecular orbitals (LUMOs) are mainly on the benzofuran ring. Thus, the ring part of these models is considered as the reactive site. The molecule (−)-BPAP was too big for the calculations and then the model BF1 was used mainly for the calculations and the notation of its atoms as shown in Figure 2. Table 1 represents the comparison of the optimized results by the different methods for the configurations of BF1 and BF3. It was found that the calculational results agreed well with the X-ray diffraction result.[9] It is hard to say which of the methods of calculation was better. As far as the configurations are concerned, HF/3-21G represents the easiest method well. In torsion angles of the chain part, there were some differences among the results, because of the existence of many equilibrium states due to the chain rotations, of which the energy levels were almost the same. These differences were not of concern in our calculations, because the chemically reactive site was found in the benzofuran ring as mentioned above. In consideration of the importance of the chain part, including atom N, from a pharmacological point of view, the model BF1 was chosen for the study. However, as expected, the results using the models BF2 and BF3 for the reactivities of the benzofuran ring, were similar to those using BF1.

Primary ·OH trapping products

Figure 3 represents the products a, b, c, d, e, f, g and h which are the optimized ·OH-adducts on C1, C2, C4, C5, C6, C7, C8 and C3 of the model BF1, respectively. The trapped ·OH is designated Oa-Ha in the figure. The torsion angles α = C2-C3-C8-C7 are written in the figure, which indicate that these products keep flat conformations of the ring part, except the products g and h. The bond lengths between the ring atoms for all the products are tabulated at the bottom of Figure 3. It was observed that the ·OH trappings on C1, C2, C4, C5, C6 and C7 did not change the conformation of the benzofuran ring, and that on the other hand the trappings on the angular C3 and C8, bent the benzofuran ring at an angle of 30 to 35 degrees. The energy diagrams of these products are shown in Figure 4, where the energy level of the starting reactants (BF1 + ·OH) is taken as the energy base line. The product a was decidedly at the lowest energy level (−28.87 kcal/mol) and the product h was higher by 4.25 kcal/mol than the reactants. The other products are more or less at the same energy levels (ca. −10 kcal/mol).

Generally there are two reaction types of ·OH, one is the hydrogen abstraction from the substrate by ·OH, and the other is the ·OH trapping on the substrate as treated here. As the examples of the hydrogen abstraction, case-1 for H1 on C2 and case-2 for H12 on N of the side chain part have been examined using the model BF2 for case-1 and the model BF1 for case-2. The energy levels of the respective hydrogen abstracted products with one molecular water were higher by 12.97 kcal/mol for case-1, and lower by 9.01 kcal/mol for case-2 than the energy base line of the reactants. Thus, the hydrogen abstraction reaction from the ring part were considered very unlikely. The hydrogen abstracted product from the amine together with water was higher by 19.86 kcal/mol at the energy level than the ·OH trapping product on C1 (product a), which was −28.87 kcal/mol. This result suggests that the ·OH trappings on the ring part may occur preferentially and the hydrogen abstraction from the amine would take place with them unrelatedly. The hydrogen abstraction reactions of ·OH were separated from the ·OH trapping reactions on the ring part in the present study.

Transition states

The transition states TSa, TSb, TSc, TSd, TSe, TSf and TSg for the products a, b, c, d, e, f and g are shown in Figure 5. For the product h, of which the energy level was higher than the reactants (Fig. 4), it was considered not to be worth finding the transition state. As shown in Figure 4, the activation energies for the transition states for these ·OH trappings were only about 10 kcal/mol, among which TSa or TSc was the lowest barrier. Thus, in consideration of the energy levels of the products, the route to the most stable product a via TSa, that is the ·OH trapping on C1, seems of the most occurrence. Interestingly, in the TSa, the distance between the attacked carbon C1 and the oxygen (Oa) of ·OH was much longer (2.038Å) than those in the other TSs (around 1.85Å).

Secondary reactions

Since the primary ·OH trapping products are still in radical states, they can react readily with further ·OH. As any transition states for the secondary trapping processes were not found, these radical–radical reactions

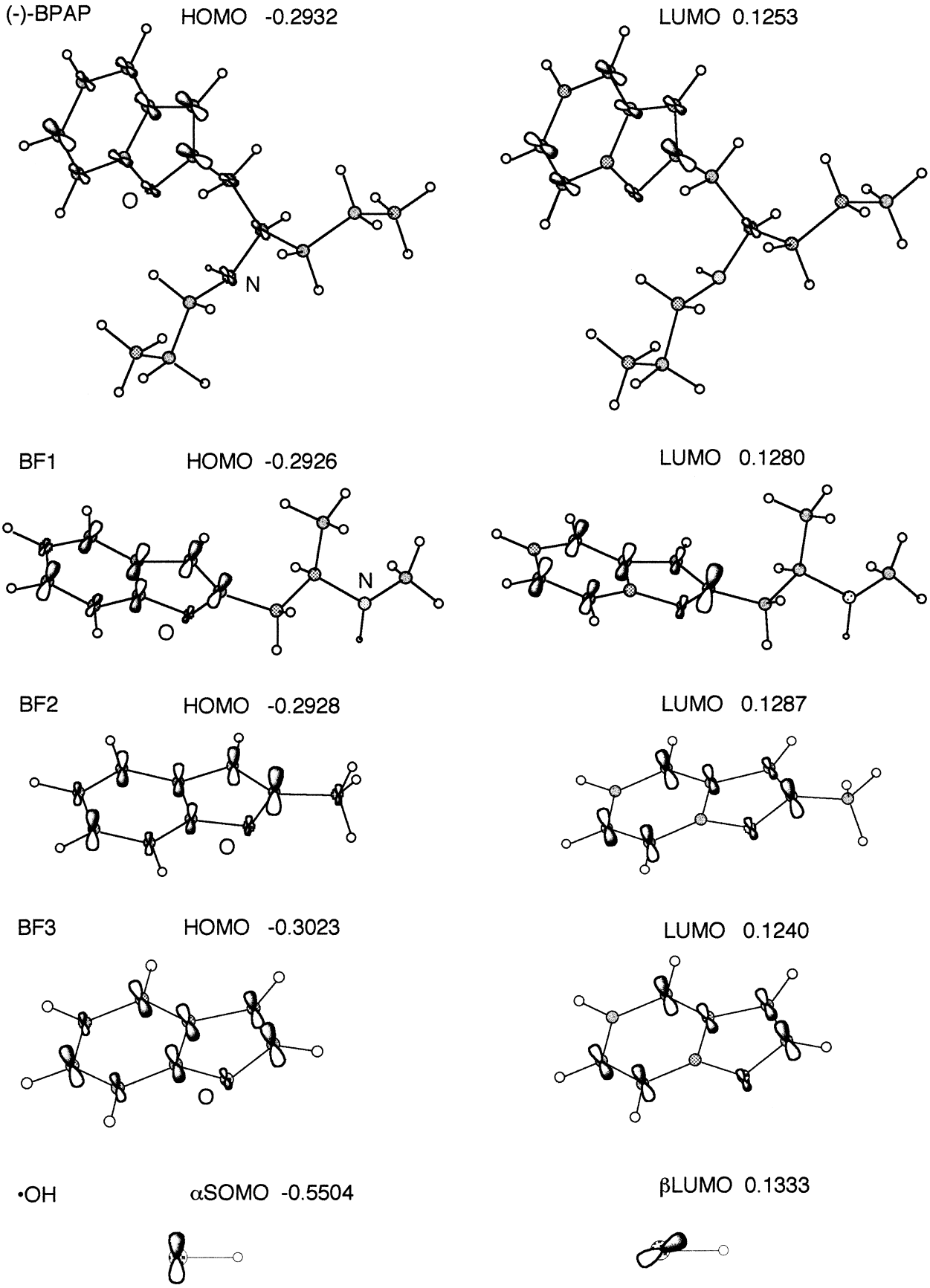

Figure 1. Configurations and frontier molecular orbitals of the reactants. The numbers are the energy levels in atomic unit.

were considered to arise by way of cascade without overcoming the reaction barrier. Simply, 28 different combinations can be mathematically considered for these double •OH trappings. However, in the present study, some representative double •OH trapping products were calculated (Fig. 6) and their energy levels are shown in Figure 4. As shown in Figure 4, the product ab, the double radical trapping product on C1 and C2, was undoubtedly at the lowest energy level (−76.1 kcal/mol). Thus, whichever primary trapping occurs on C1

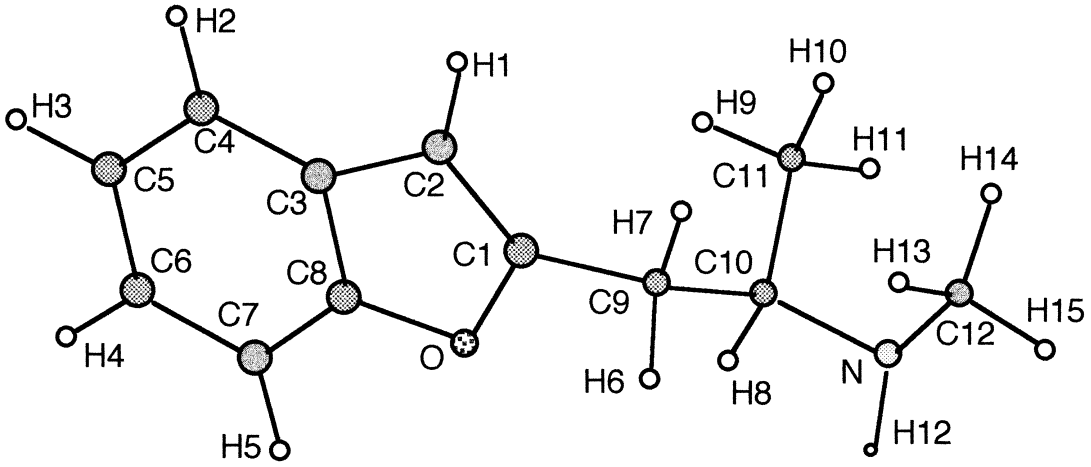

Figure 2. Notations on model BF1.

Table 1. Comparison of the configurational results with the differnt models and methods

Model	(−)-BPAP	BF1		BF3			
Method	Exp.[a]	HF/3-21G	HF/6-31G(d)	HF/3-21G	MP2/3-21G	MP2/6-31G(d)	B3LYP/3-21G
Bond lengths							
C1-C2	1.339	1.338	1.338	1.334	1.368	1.361	1.356
C2-C3	1.440	1.457	1.450	1.458	1.461	1.438	1.454
C3-C4	1.392	1.388	1.392	1.388	1.413	1.405	1.401
C4-C5	1.371	1.381	1.381	1.379	1.400	1.390	1.393
C5-C6	1.369	1.396	1.398	1.397	1.422	1.411	1.408
C6-C7	1.375	1.382	1.382	1.380	1.401	1.392	1.395
C7-C8	1.370	1.376	1.381	1.378	1.401	1.393	1.388
C3-C8	1.389	1.388	1.388	1.389	1.418	1.407	1.412
C8-O	1.371	1.379	1.352	1.378	1.413	1.372	1.398
O-C1	1.381	1.397	1.361	1.394	1.429	1.376	1.414
C1-C9	1.481	1.492	1.492				
C9-C10	1.510	1.539	1.549				
C10-C11	1.530	1.536	1.528				
N-C10	1.516	1.473	1.457				
N-C12	1.484	1.469	1.450				
Bond angles							
C1-C2-C3	107.3	107.25	106.32	106.63	106.82	105.98	106.87
C2-C3-C4	136.2	134.75	136.02	134.66	134.59	135.75	134.72
C3-C4-C5	118.0	118.37	118.43	118.34	118.32	118.28	118.38
C4-C5-C6	121.7	121.11	121.14	121.08	121.28	121.48	121.27
C5-C6-C7	121.8	121.08	121.22	121.17	121.22	121.39	121.16
C6-C7-C8	116.5	116.86	116.56	116.88	116.74	116.12	116.91
C2-C3-C8	105.0	105.88	104.87	105.88	106.22	105.52	106.09
C4-C3-C8	118.8	119.37	119.10	119.46	119.19	118.73	119.19
C7-C8-O	126.2	127.47	126.26	127.31	126.49	125.53	127.03
C3-C8-O	110.5	109.32	110.19	109.63	110.27	110.49	109.88
C3-C8-C7	123.3	123.21	123.55	123.06	123.24	123.99	123.09
C1-O-C8	106.0	107.22	107.15	106.49	104.93	105.65	105.57
O-C1-C2	111.2	110.33	111.47	111.37	111.76	112.36	111.59
O-C1-C9	115.9	114.72	115.83				
C2-C1-C9	132.9	134.92	132.70				
C1-C9-C10	112.5	114.10	113.90				
C9-C10-C11	113.8	110.30	111.93				
N-C10-C9	109.2	106.90	113.57				
N-C10-C11	110.3	109.73	110.90				
C10-N-C12	117.2	116.38	118.17				

[a]The experimental results of X-ray diffraction of (−)-BPAP.[9]

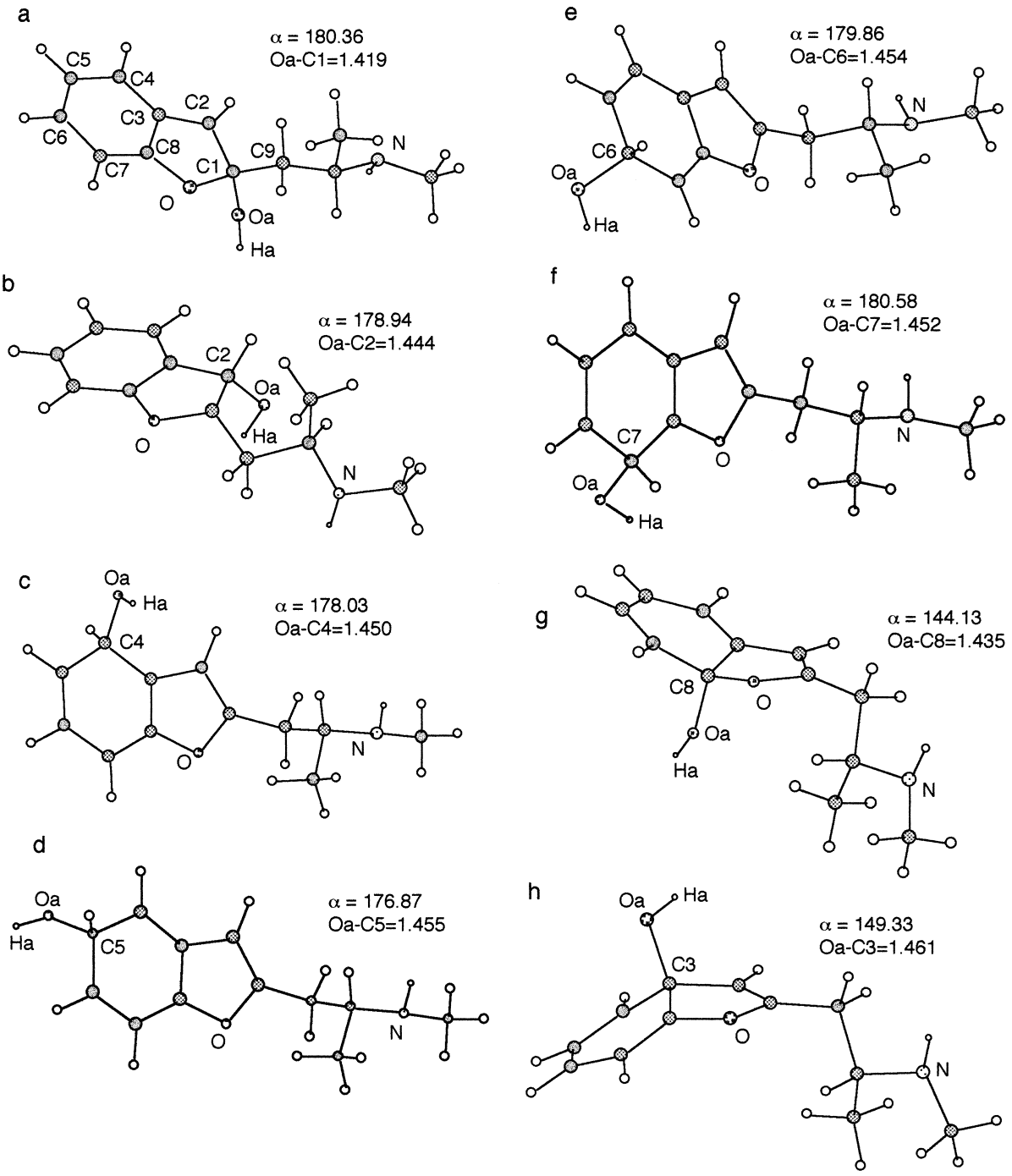

bond length	a	b	c	d	e	f	g	h
C1-C2	1.519	1.529	1.366	1.354	1.367	1.353	1.366	1.320
C2-C3	1.398	1.515	1.424	1.448	1.426	1.447	1.424	1.518
C3-C4	1.412	1.376	1.497	1.381	1.420	1.421	1.388	1.501
C4-C5	1.395	1.389	1.443	1.511	1.366	1.416	1.404	1.375
C5-C6	1.405	1.388	1.375	1.519	1.513	1.379	1.428	1.421
C6-C7	1.410	1.387	1.423	1.376	1.514	1.512	1.372	1.419
C7-C8	1.372	1.374	1.395	1.398	1.354	1.483	1.493	1.362
C3-C8	1.419	1.380	1.384	1.413	1.422	1.372	1.511	1.510
C8-O	1.387	1.384	1.385	1.387	1.391	1.385	1.439	1.403
O-C1	1.462	1.423	1.402	1.407	1.408	1.403	1.414	1.415
C1-C9	1.529	1.494	1.489	1.490	1.489	1.490	1.485	1.487

Figure 3. Primary •OH trapping products. The numbers are in Å for the bond lengths and in degrees for the angles, α = C2-C3-C8-C7.

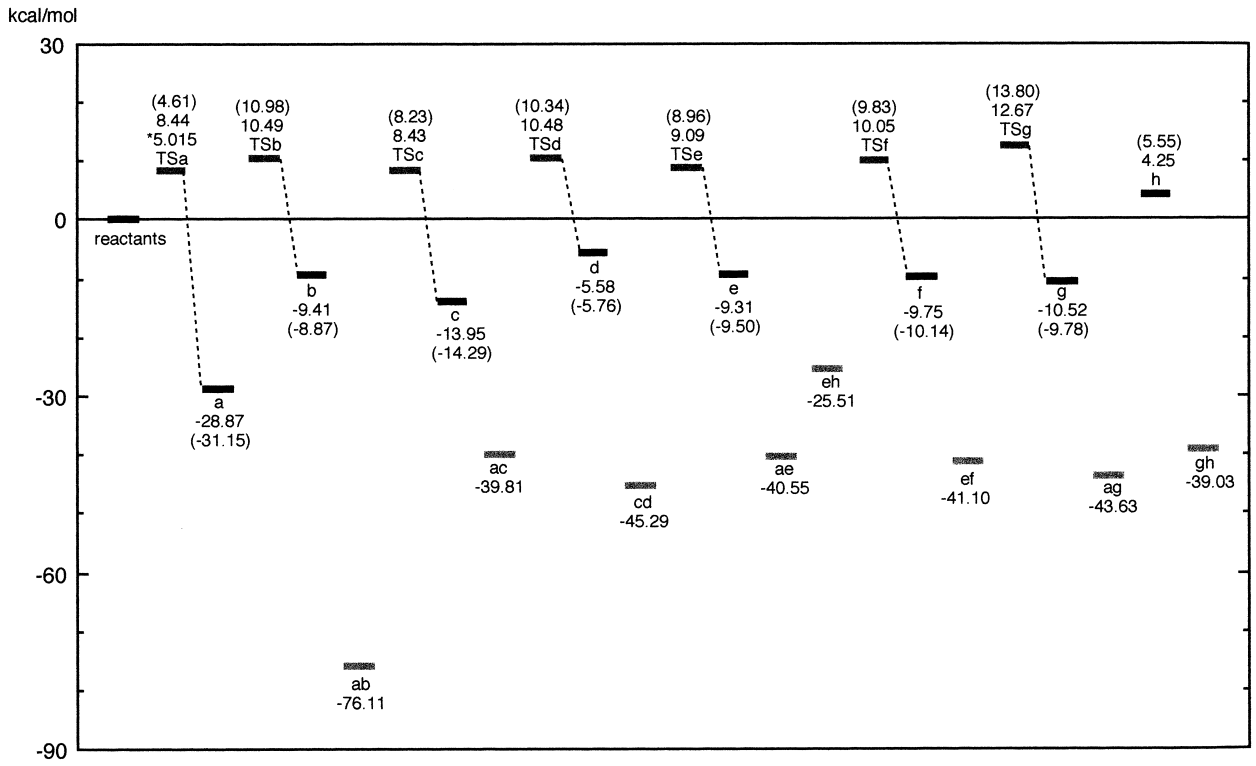

Figure 4. Energy diagrams of all products. The numbers are energy differences from the reactants level in kcal/mol. The numbers in parentheses are the results using smaller models BF2 and BF3; BF2 for a, b, g, h and their transition states and BF3 for c, d, e, f and their transition states. * Optimized at UHF/6-31G(d) level.

(product a) or on C2 (product b), the secondary trapping will readily take place on C2 or C1 to give the same product. The energy levels of most of the other double trapping products were lower than the energy base line by around 40 kcal/mol.

It is considered that the above double trapping products will undergo further changes. As one such reaction, the reaction of Oa-Ha on C1 with H1 on C2 in the product ab leading to the dehydration was studied. As a result, the dehydrated product together with water was higher however at the energy level by 16.80 kcal/mol than the product ab. The more theoretical and experimental verifications, which have not been carried out yet, will be necessary to discuss the final dehydrated products. Thus, further pursuit is not included in the present study.

Figure 7 shows the singly occupied molecular orbitals (SOMOs) of the primary •OH trapping products, and Table 2 represents the spin density distributions of them. It was noticed that the alternative sign spins appeared in the ring carbons and that generally the atoms with large orbital lobes in the SOMOs correspond to the atoms with positive sign spins which could possibly trap the second •OH.

Spin and charge variations

Table 2 represents the spin density distributions of all the radical states and Table 3 shows the atomic charge density distributions of all species calculated, listing only the values for the ring atoms and atom C9 in the chain part. Figure 8 graphically shows the spin and charge densities of all atoms of product a as a representative example. It was observed that the spins were assembled in the ring part and that there was practically no spins in the chain part. The charge densities on the atoms of the chain part were almost unchanged during the reaction process.

Initially the spin values of •OH were 1.057 on Oa and −0.057 on Ha. It was interesting to find in Table 2 that the spin on Oa changed from this value, 1.057, passing through the transition states (ca. 0.7 to 0.8) to almost zero value of the products, meaning that the spin was totally transferred from the •OH side toward the benzofuran side. In the case of product b, there was no large spin on the benzene ring and the spin was totally localized on the atom C1 of the furan ring. The spin densities on the benzene ring in TSb, of which the magnitudes were smaller than the ones of the other TSs, were once distributed but disappeared in the process from TSb to product b. This phenomenon was odd but the same one was observed also in the smaller model systems BF2 + •OH and BF3 + •OH.

Alternatively, the charge density (Table 3) on Oa of •OH was −0.441 in electron unit at the beginning, and it became about −0.6 in the transition states and then was about −0.75 in the single •OH trapping products. In the double trapping products the charges on Oa and Ob (O of the secondary •OH) were both about −0.8. Inversely, the charge densities on the carbon atoms connected with

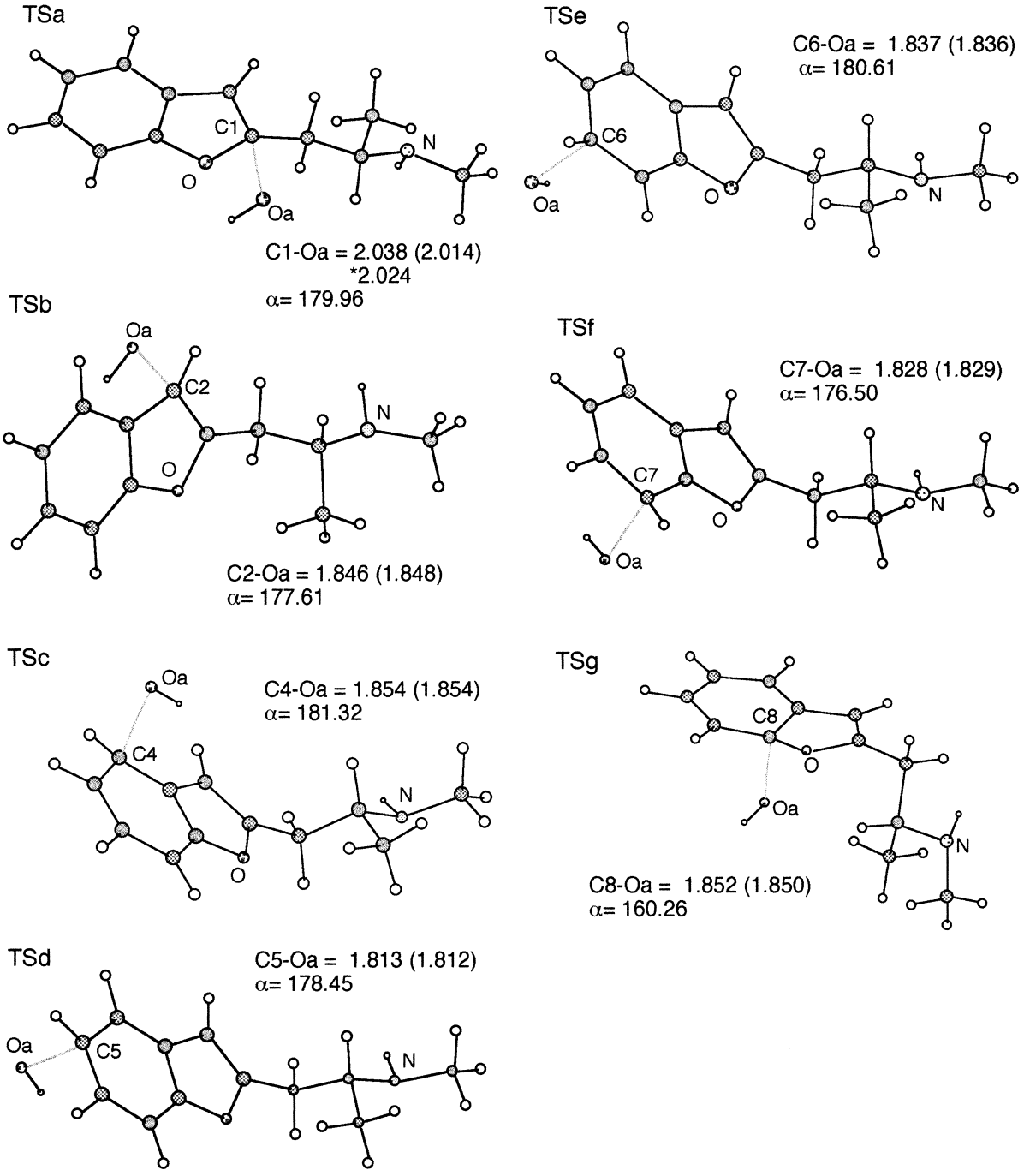

bond length	TSa	TSb	TSc	TSd	TSe	TS f	TSg
C1-C2	1.409	1.419	1.359	1.354	1.360	1.354	1.360
C2-C3	1.424	1.466	1.434	1.446	1.436	1.445	1.433
C3-C4	1.405	1.394	1.436	1.393	1.411	1.410	1.393
C4-C5	1.395	1.396	1.443	1.446	1.384	1.406	1.404
C5-C6	1.404	1.401	1.392	1.451	1.450	1.395	1.414
C6-C7	1.404	1.400	1.411	1.390	1.445	1.447	1.391
C7-C8	1.377	1.380	1.388	1.391	1.372	1.423	1.425
C3-C8	1.408	1.399	1.396	1.408	1.411	1.391	1.445
C8-O	1.388	1.387	1.385	1.385	1.388	1.383	1.398
O-C1	1.429	1.414	1.404	1.406	1.406	1.401	1.411
C1-C9	1.507	1.488	1.489	1.490	1.489	1.490	1.485

Figure 5. Transition states for the primary •OH trappings. The numbers are in Å for the bond lengths and in degrees for the angles, α = C2-C3-C8-C7. The numbers in parentheses are the results using smaller models BF2 and BF3. * Optimized at UHF/6-31G(d) level.

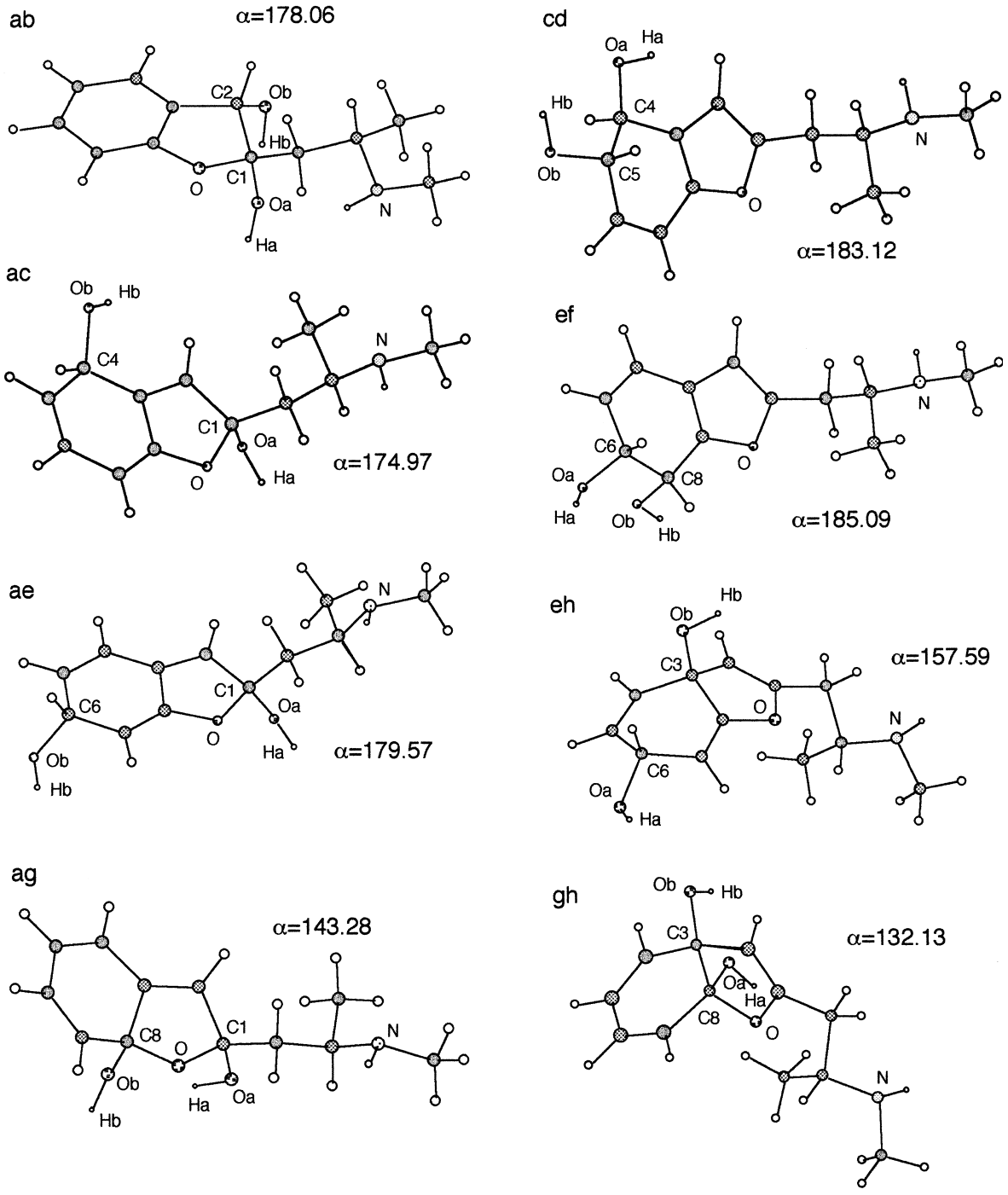

bond length	ab	ac	ae	ag	cd	ef	eh	gh
C1-C2	1.555	1.519	1.519	1.531	1.347	1.345	1.320	1.311
C2-C3	1.513	1.321	1.321	1.317	1.440	1.446	1.514	1.519
C3-C4	1.371	1.455	1.455	1.454	1.496	1.465	1.508	1.505
C4-C5	1.392	1.322	1.322	1.330	1.530	1.322	1.314	1.319
C5-C6	1.385	1.512	1.512	1.477	1.514	1.521	1.516	1.473
C6-C7	1.391	1.512	1.512	1.324	1.324	1.542	1.516	1.318
C7-C8	1.370	1.313	1.313	1.496	1.454	1.483	1.305	1.493
C3-C8	1.377	1.468	1.468	1.512	1.342	1.338	1.520	1.572
C8-O	1.395	1.380	1.380	1.421	1.371	1.378	1.400	1.446
O-C1	1.447	1.461	1.461	1.460	1.393	1.389	1.412	1.408
C1-C9	1.514	1.530	1.530	1.519	1.489	1.490	1.486	1.487

Figure 6. Secondary trapping products.

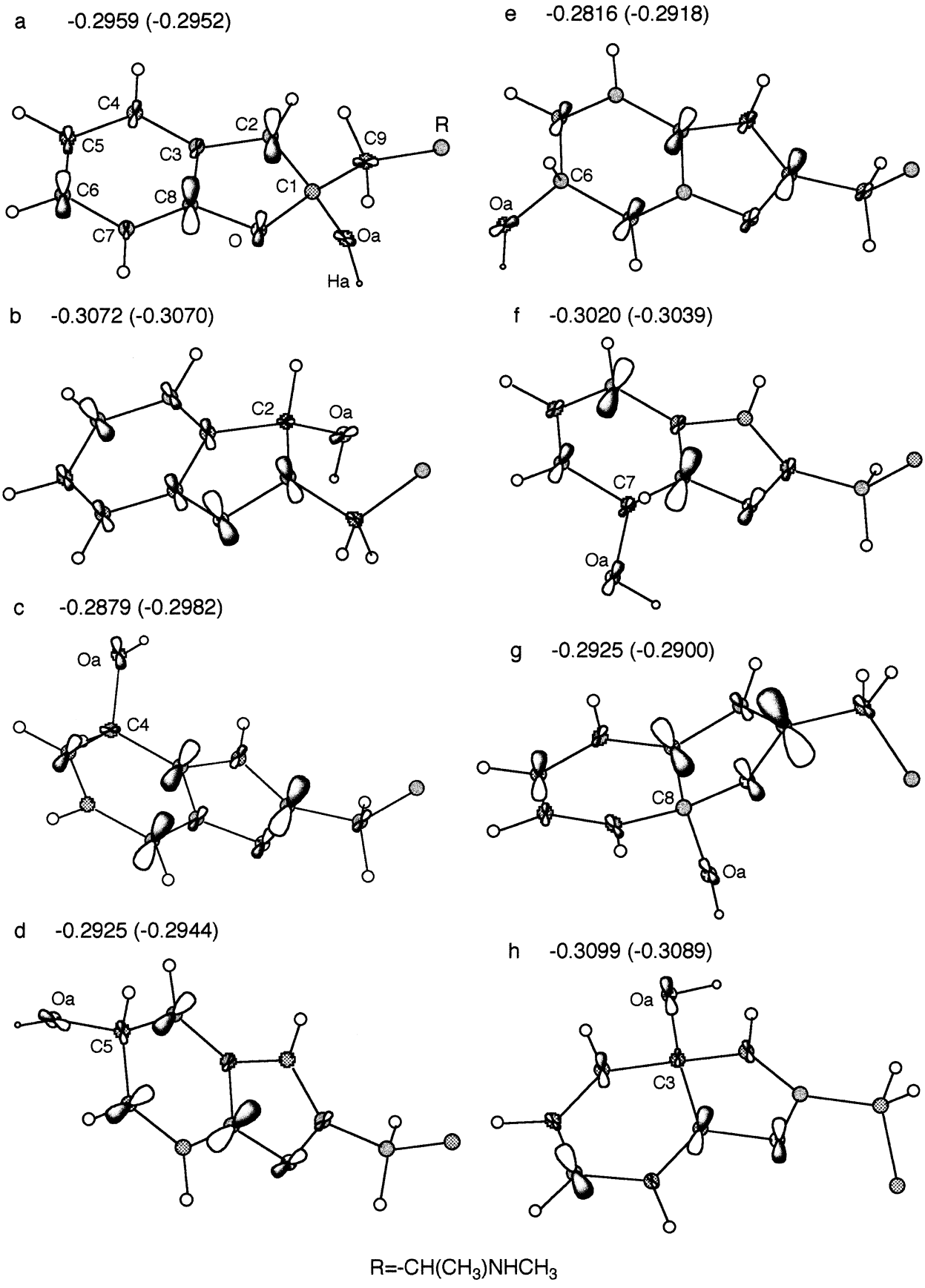

Figure 7. SOMOs of the primary •OH trapping products. The numbers are energy levels in atomic unit and those using smaller models in parentheses.

Table 2. The spin densities of the primary •OH trapping products and the transition states

	TSa	a	TSb	b	TSc	c	TSd	d	TSe	e	TSf	f	TSg	g	h
C1	−0.742	−0.117	0.969	1.087	0.614	0.651	−0.582	−0.601	0.642	0.721	−0.546	−0.533	0.695	0.770	−0.002
	−0.146	−0.048	0.578	0.853	0.139	0.200			0.196	0.301					
C2	0.430	1.078	−0.663	−0.107	−0.601	−0.613	0.591	0.616	−0.628	−0.688	0.551	0.543	−0.678	−0.742	0.033
	0.923	0.741	−0.155	−0.056	−0.082	−0.104			−0.111	−0.162					
C3	−0.759	−0.819	0.694	−0.023	0.779	0.781	−0.774	−0.821	0.816	0.902	−0.740	−0.745	0.865	0.943	−0.208
	−0.131	−0.230	0.055	0.026	0.224	0.279			0.280	0.399					
C4	0.782	0.845	−0.704	0.038	−0.695	−0.189	0.940	1.031	−0.803	−0.795	0.907	1.026	−0.845	−0.888	0.944
	0.141	0.279	−0.031	−0.003	−0.175	−0.061			−0.169	−0.186					
C5	−0.730	−0.775	0.676	−0.039	0.873	0.916	−0.661	−0.234	0.852	0.879	−0.798	−0.830	0.876	0.969	−0.825
	−0.078	−0.141	0.030	0.012	0.365	0.464			0.271	0.328					
C6	0.772	0.836	−0.696	0.039	−0.806	−0.816	0.892	0.943	−0.676	−0.204	0.892	0.950	−0.826	−0.820	0.990
	0.149	0.290	−0.026	−0.000	−0.197	−0.239			−0.172	−0.070					
C7	−0.710	−0.735	0.659	−0.041	0.852	0.969	−0.782	−0.801	0.841	0.874	−0.655	−0.189	0.880	0.917	−0.817
	−0.082	−0.126	0.024	0.007	0.393	0.576			0.386	0.512					
C8	0.670	0.724	−0.607	0.030	−0.691	−0.715	0.764	0.856	−0.688	−0.696	0.738	0.757	−0.601	−0.190	0.861
	0.121	0.204	−0.025	−0.004	−0.141	−0.177			−0.152	−0.197					
C9	0.089	0.018	−0.138	−0.134	−0.084	−0.090	0.078	0.081	−0.088	−0.100	0.073	0.071	−0.094	−0.106	−0.001
	0.017	0.019	−0.058	−0.076											
O	0.006	0.009	0.000	0.010	−0.002	−0.000	0.004	0.006	−0.002	−0.002	0.007	0.009	−0.003	0.006	−0.016
	−0.010	0.026	0.064	0.088	0.012	0.018			0.014	0.028					
Oa	0.852	0.019	0.710	0.037	0.719	0.047	0.665	0.045	0.691	0.043	0.694	0.050	0.684	0.056	0.066
	0.646	0.023	0.480	0.050	0.485	0.047			0.479	0.045					
Ha	−0.041	0.004	−0.035	−0.001	−0.035	0.004	−0.033	0.003	−0.034	0.003	−0.033	0.001	−0.032	0.005	0.005
	−0.021	0.007	−0.013	0.002	−0.013	0.006			−0.013	0.005					
S^2	1.698	1.080	1.416	0.750	1.483	1.055	1.508	1.138	1.481	1.081	1.435	1.039	1.697	1.281	0.901
	1.535[a]														

[a]Optimized at UHF/6-31G(d) level. The second lines are the results by the method UB3LYP/3-21G//UHF/3-21G level with smaller models. The underlines indicate the atoms connected with •OH.

Table 3. The atomic charge densities of the primary •OH trapping products and the transition states[a]

	TSa	a	TSb	b	TSc	c	TSd	d	TSe	e	TSf	f	TSg	g	h
C1	0.382	0.649	0.378	0.335	0.364	0.362	0.371	0.372	0.370	0.367	0.375	0.374	0.391	0.402	0.416
C2	−0.176	−0.224	−0.146	0.139	−0.253	−0.261	−0.263	−0.262	−0.262	−0.258	−0.270	−0.273	−0.262	−0.265	−0.322
C3	−0.039	−0.018	−0.034	−0.127	−0.009	−0.098	−0.041	−0.006	−0.048	−0.057	−0.057	−0.037	0.027	0.010	0.219
C4	−0.190	−0.187	−0.190	−0.192	−0.131	0.172	−0.170	−0.209	−0.194	−0.166	−0.191	−0.195	−0.184	−0.183	−0.158
C5	−0.208	−0.208	−0.211	−0.226	−0.169	−0.232	−0.109	0.131	−0.167	−0.190	−0.211	−0.186	−0.200	−0.202	−0.180
C6	−0.204	−0.201	−0.202	−0.188	−0.211	−0.185	−0.173	−0.224	−0.121	0.132	−0.170	−0.193	−0.186	−0.181	−0.201
C7	−0.238	−0.243	−0.239	−0.256	−0.232	−0.237	−0.230	−0.198	−0.215	−0.290	−0.150	0.131	−0.202	−0.207	−0.232
C8	0.383	0.407	0.402	0.443	0.382	0.395	0.382	0.364	0.395	0.434	0.415	0.321	0.423	0.584	0.392
C9	−0.384	−0.380	−0.373	−0.360	−0.365	−0.364	−0.365	−0.365	−0.365	−0.365	−0.365	−0.364	−0.372	−0.374	−0.370
O	−0.727	−0.749	−0.700	−0.702	−0.696	−0.695	−0.697	−0.700	−0.700	−0.708	−0.680	−0.693	−0.699	−0.720	−0.701
Oa	−0.570	−0.753	−0.617	−0.757	−0.609	−0.756	−0.634	−0.753	−0.623	−0.753	−0.614	−0.754	−0.620	−0.738	−0.754
Ha	0.454	0.448	0.434	0.439	0.432	0.434	0.429	0.432	0.430	0.434	0.430	0.446	0.426	0.438	0.433

The atomic charge densities of the double •OH trapping products and the reactants

	BF1+•OH	ab	ac	ae	ag	cd	ef	eh	gh
C1	0.374	0.609	0.638	0.645	0.656	0.368	0.375	0.423	0.450
C2	−0.274	0.189	−0.229	−0.268	−0.253	−0.284	−0.288	−0.335	−0.341
C3	−0.046	−0.113	−0.068	−0.004	0.015	−0.144	−0.056	0.216	0.270
C4	−0.206	−0.198	0.186	−0.156	−0.144	0.175	−0.144	−0.157	−0.145
C5	−0.215	−0.222	−0.269	−0.183	−0.216	0.170	−0.233	−0.172	−0.203
C6	−0.209	−0.191	−0.158	0.140	−0.171	−0.228	0.172	0.134	−0.185
C7	−0.241	−0.258	−0.326	−0.347	−0.219	−0.181	0.103	−0.301	−0.175
C8	0.399	0.444	0.489	0.489	0.580	0.360	0.299	0.446	0.620
C9	−0.359	−0.345	−0.380	−0.380	−0.375	−0.365	−0.365	−0.371	−0.368
O	−0.690	−0.734	−0.743	−0.748	−0.723	−0.666	−0.666	−0.704	−0.719
Oa		−0.800	−0.750	−0.750	−0.780	−0.781	−0.787	−0.764	−0.801
Ha		0.464	0.451	0.450	0.473	0.438	0.476	0.438	0.458
Ob	−0.441	−0.772	−0.756	−0.757	−0.770	−0.780	−0.784	−0.756	−0.790
Hb	0.441	0.473	0.434	0.437	0.443	0.455	0.453	0.434	0.483

[a]Those of the reactant •OH are in Ob and Hb of the column BF1+•OH. The underlines indicate the atoms connected with •OH.

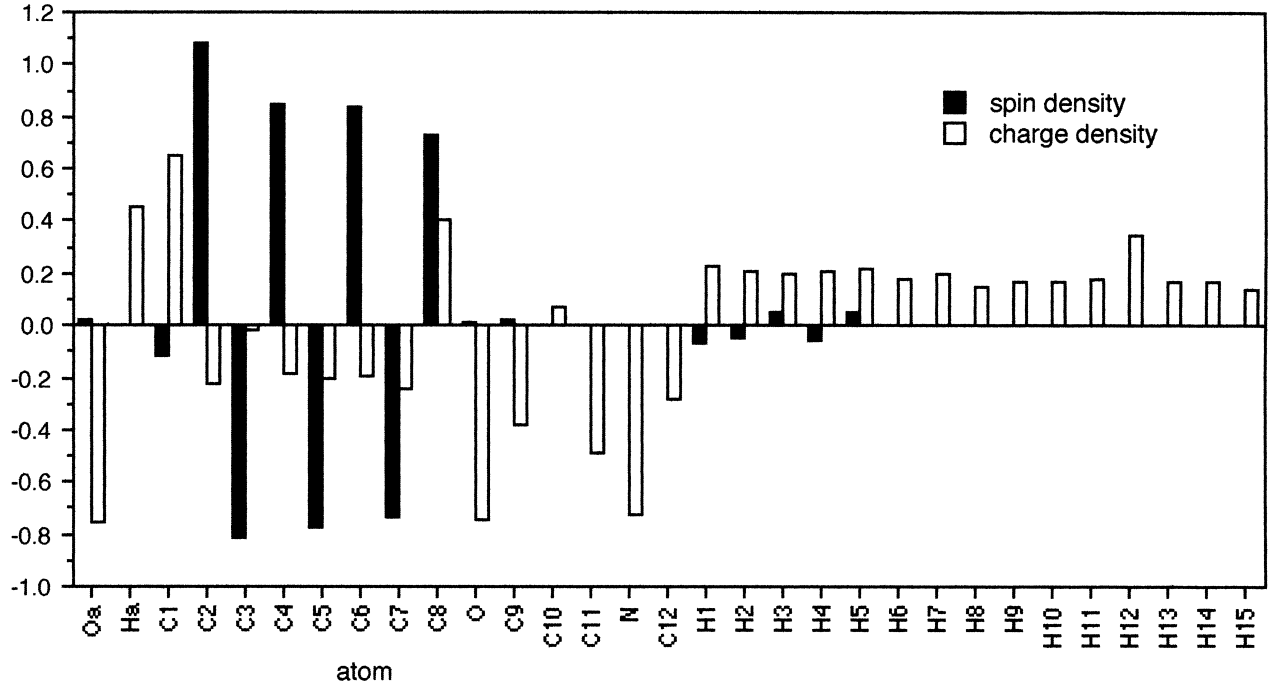

Figure 8. The spin and charge densities of product a.

Table 4. Comparison of the higher order calculational results by methods B and C with the result by method A for TSc using model BF3

Method	UHF A	UMP2 B	UB3LYP C
Spin density			
C1	0.642	0.524	0.038
C2	−0.624	−0.529	−0.015
C3	0.777	0.733	0.072
C4	−0.699	−0.730	−0.035
C5	0.875	0.820	0.175
C6	−0.807	−0.756	−0.082
C7	0.855	0.797	0.157
C8	−0.691	−0.656	−0.049
O	0.003	0.001	0.015
Oa	0.721	0.851	0.755
Ha	−0.035	−0.046	−0.023
Charge density			
C1	0.123	0.128	0.084
C2	−0.243	−0.234	−0.198
C3	−0.006	−0.001	0.136
C4	−0.131	−0.201	−0.189
C5	−0.169	−0.165	−0.088
C6	−0.211	−0.219	−0.154
C7	−0.228	−0.221	−0.173
C8	0.376	0.368	0.311
O	−0.658	−0.670	−0.497
Oa	−0.607	−0.546	−0.533
Ha	0.433	0.434	0.370
S^2	1.523	1.358	0.750
Activation energy	8.23	29.35	−3.75
Bond length			
C1-C2	1.359	1.325	1.358
C2-C3	1.436	1.474	1.450
C3-C4	1.437	1.420	1.411
C4-C5	1.443	1.414	1.412
C5-C6	1.393	1.392	1.406
C6-C7	1.411	1.387	1.396
C7-C8	1.389	1.398	1.392
C3-C8	1.397	1.379	1.408
C8-O	1.383	1.401	1.396
O-C1	1.398	1.416	1.414
Oa-C4	1.855	1.952	2.143

•OH were higher by about 0.3 than those of the other carbon atoms. Thus, on the •OH trapping process, it is considered that the charge moved from the carbon atom connected with •OH toward the oxygen atom of •OH, in the opposite direction to the spin movement.

Higher order calculations

The S^2 values for all radical states calculated are shown in the bottom row of Table 2. The values of about 1.0–1.7 were too large to 0.75 (no spin contamination), all the calculational results having too much spin contamination. This did not improve much even if the basis set for the optimizations was changed from 3-21G to 6-31G(d) (Table 2). In order to know the effect of the calculational method, we recalculated TSc and product c by methods B and C, using a smaller model BF3. Table 4 represents comparison of the results for TSc by each method, showing the charge densities, the spin densities, S^2 values, the activation energies and the bond lengths. Method B did not alter the characteristics of the results by method A, except for the activation energy (29.35 versus 8.23 kcal/mol). The configurational results by method C were similar to the ones by methods A and B, except that the distance C4-Oa was very long (2.143Å) even though checked by the frequency analysis. A further important point in the result by method C was that the activation energy for TSc was −3.75 kcal/mol, which was not realistic. Accordingly, the results by method A are considered appropriate from an energetical point of view. This is also deduced from the close results for TSa; 8.44 kcal/mol by method A versus 5.01 kcal/mol optimized at UHF/6-31G(d) level (see Fig. 4).

In the meantime, Figure 9 represents the graphical comparisons of the spin and charge density distribu-

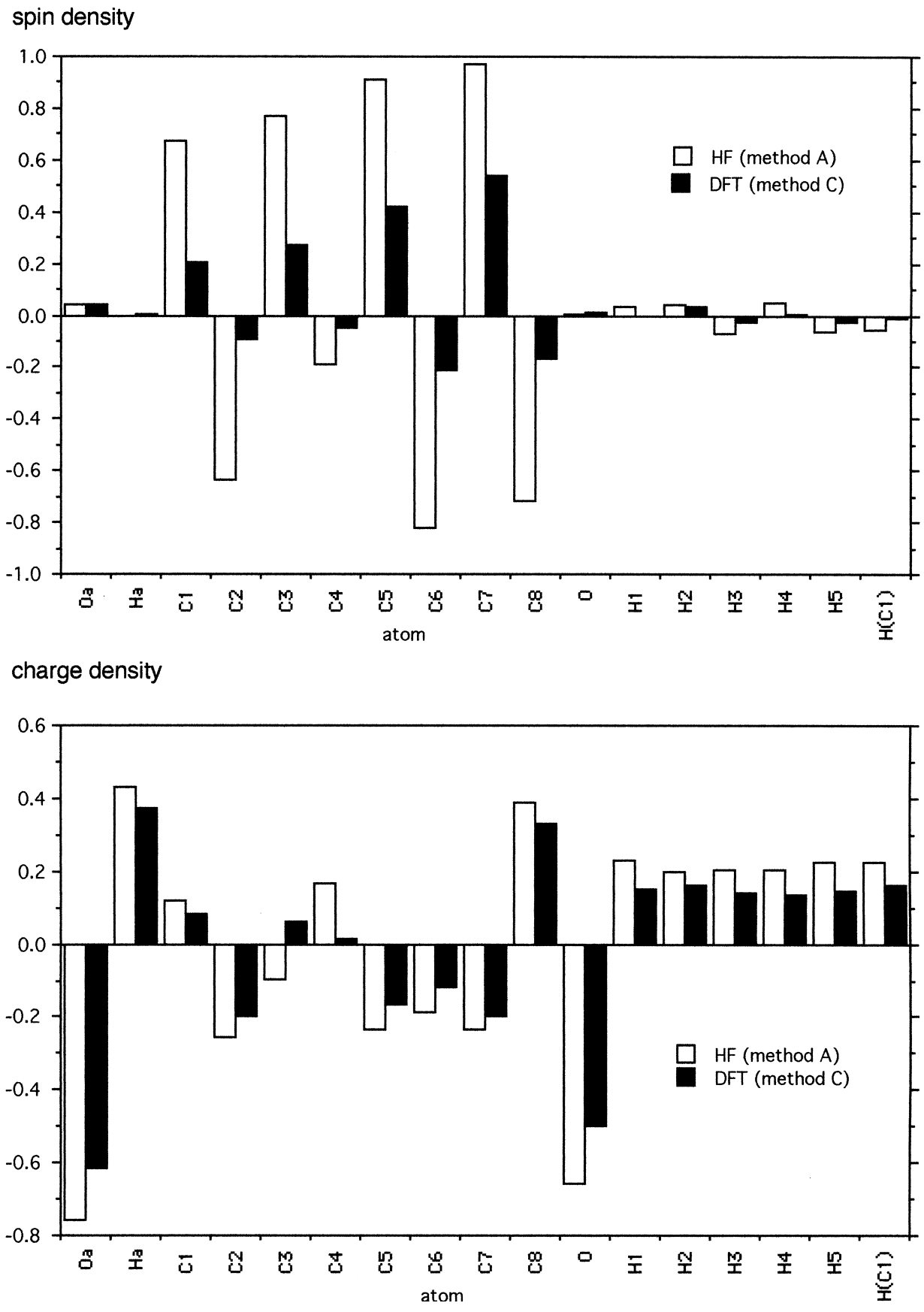

Figure 9. The spin and charge densities of product c using model BF3 by HF (method A) and DFT (method C). The result by MP2 (method B) was similar to the one by HF.

tions for product c by methods A and C using model BF3. The results by both methods displayed a similar tendency, but the charge densities by method C were slightly smaller than those by method A, while the spin densities by method C were considerably smaller than those by method A. This can also be seen in the density distributions in Table 4 for TSc. Thus, method C gave good S^2 values around 0.75 for product c and TSc, probably by giving good density distributions.

It is concluded that the values for the spin density presented in Table 2 were qualitatively correct but quantitatively much exaggerated. Also, the values in Table 3 for the charge densities have to be regarded with a little discount. In order to get the realistic spin density distributions, the single point calculations with the method UB3LYP/3-21G//UHF/3-21G level for some of the primary products and transition states were carried out using smaller models BF2 and BF3. The results are presented in the second lines in Table 2, noting that the activation energies obtained by this method were all minus as in the case for TSc by method C (Table 4).

Conclusion

Possible reaction mechanisms of (−)-BPAP with •OH have been investigated by the molecular orbital theory using the simplified models. Thus, product a (•OH adduct on C1) for the primary •OH trapping and product ab (double •OH adduct on C1 and C2) for the secondary trapping have been found to be generated predominantly from viewpoints of energy levels of the products. However, the calculated results indicated that many other •OH trapping products could be formed concomitantly with the above main products. The formation of the secondary products and their structures can be predicted through the spin density distributions and the SOMOs of the primary •OH trapping products.

Our previous study made it clear that (−)-deprenyl was a good scavenger of •OH, the active site being the acetylenic part.[1] The present study suggested that (−)-BPAP has higher potency than (−)-deprenyl in scavenging •OH from the viewpoint of the energy levels of the products, and the active site of this reaction is on the benzofuran ring. Thus, it is theoretically concluded that (−)-BPAP may be useful as a neuroprotective drug, scavenging the toxic •OH radical for the neurodegenerative diseases concerned with possible oxidative damages in the CNS, such as Parkinson's disease, senile dementia and Alzheimer's disease.

References

1. Nakai, S.; Yoneda, F. *Theor. Chem. Acc* **2000**, *104*, 398.
2. (a) Knoll, J.; Miklya, I.; Knoll, B.; Markó, R.; Klemen, K. *Life Sci*. **1996**, *58*, 817. (b) Knoll, J.; Miklya, I. *Life Sci*. **1995**, *56*, 611. (c) Knoll, J. *Pharmacol. Toxicol*. **1998**, *82*, 57.
3. (a) Birkmayer, B.; Riedere, P.; Youdim, M. B. H.; Linnauer, W. *J. Neural Transm*. **1975**, *36*, 303. (b) Knoll, J. *J. Neural Transm*. **1986**, *Suppl. 22*, 75.
4. (a) Knoll, J.; Yoneda, F.; Knoll, B.; Ohde, H.; Miklya, I. *Br. J. Pharmacol*. **1999**, *128*, 1723. (b) Yoneda, F.; Moto, T.; Sakae, M.; Ohde, H.; Knoll, B.; Miklya, I.; Knoll, J. *Bioorg. Med. Chem*. **2001**, *9*, (this issue).
5. (a) Okada, Y.; Kaneko, M.; Okajima, H. *Biol. Pharm. Bull*. **1996**, *19*, 1607. (b) Okada, Y.; Okajima, Y. *Yakugaku Zasshi* **1998**, *118*, 226.
6. Frisch, M. J.; Trucks, G. W.; Schlegel, H. B.; Gill, P. M. W.; Johnson, B. G.; Robb, M. A.; Cheeseman, J. R.; Keith, T.; Petersson, G. A.; Montgomery, J. A.; Raghavachari, K.; Al-Laham, M. A.; Zakrzewski, V. G.; Ortiz, J. V.; Foresman, J. B.; Cioslowski, J.; Stefanov, B. B.; Nanayakkara, A.; Challacombe, M.; Peng, C. Y.; Ayala, P. Y.; Chen, W.; Wong, M. W.; Andres, J. L.; Replogle, E. S.; Gomperts, R.; Martin, R. L.; Fox, D. J.; Binkley, J. S.; Defrees, D. J.; Baker, J.; Stewart, J. P.; Head-Gordon, M.; Gonzalez, C.; Pople, J. A. *Gaussian 94,* Revision E.3; Gaussian, Inc.: Pittsburgh, PA, 1995.
7. (a) Møller, C.; Plesset, M. S. *Phys. Rev*. **1934**, *46*, 618. (b) Handy, C.; Schaefer, H. F., III *J. Chem. Phys*. **1984**, *81*, 5031. (c) Frisch, M. J.; Head-Gordon, M.; Pople, J. A. *Chem. Phys. Lett*. **1990**, *166*(3), 281.
8. (a) Lee, C.; Yang, W.; Parr, R. G. *Phys. Rev. B* **1988**, *37*, 785. (b) Beck, A. D. *J. Chem. Phys* **1993**, *98*, 5648. Oka, T.; Yasusa, T.; Ando, T.; Watanabe, M.; Yoneda, F.; Ishida, T.; Knoll, J. *Bioorg. Med. Chem*. **2001**, *9*, (this issue).